Keisuke Uemura ORCID iD: 0000-0002-9245-1743

Andrew Anderson ORCID iD: 0000-0003-4708-2608

Prediction of Femoral Head Coverage from Articulated Statistical Shape Models of Patients with Developmental Dysplasia of the Hip

Penny R. Atkins[1,2], Praful Agrawal[1], Joseph D. Mozingo[2], Keisuke Uemura[2,3], Kunihiko Tokunaga[4], Christopher L. Peters[2], Shireen Y. Elhabian[1,7], Ross T. Whitaker[1,7], Andrew E. Anderson[1,2,5,6]

Penny R. Atkins and Praful Agrawal contributed equally to the development of this article.

1 Scientific Computing and Imaging Institute, University of Utah, Salt Lake City, Utah
2 Department of Orthopaedics, University of Utah, Salt Lake City, Utah
3 Graduate School of Information Science, Nara Institute of Science and Technology, Ikoma, Japan
4 Niigata Hip Joint Center, Kameda Daiichi Hospital, Niigata City, Japan
5 Department of Biomedical Engineering, University of Utah, Salt Lake City, Utah
6 Department of Physical Therapy and Athletic Training, University of Utah, Salt Lake City, Utah
7 School of Computing, University of Utah, Salt Lake City, Utah

Corresponding Author:

Andrew E. Anderson

590 Wakara Way, Rm A100

Salt Lake City, UT 84108

801.414.4119

Andrew.Anderson@hsc.utah.edu

Running Title: Prediction of Femoral Head Coverage

Author contributions statement: PRA, PA, JDM, KU, and AEA designed the study, PA, SYE, and RTW designed and developed software, KU and KT collected and processed

This article has been accepted for publication and undergone full peer review but has not been through the copyediting, typesetting, pagination and proofreading process, which may lead to differences between this version and the Version of Record. Please cite this article as doi: 10.1002/jor.25227.

image data, PRA, PA, JDM, KU, CLP, and AEA analyzed and interpreted the results of the study. All authors contributed to writing and revising the manuscript. All authors have read and approved the final submitted manuscript. Experimental contributions of PA were completed during his PhD and before his joining Amazon Inc. as an Applied Scientist.

Abstract

Developmental dysplasia of the hip (DDH) is commonly described as reduced femoral head coverage due to anterolateral acetabular deficiency. Although reduced coverage is the defining trait of DDH, more subtle and localized anatomic features of the joint are also thought to contribute to symptom development and degeneration. These features are challenging to identify using conventional approaches. Herein, we assessed the morphology of the full femur and hemi-pelvis using an articulated statistical shape model (SSM). The model determined the morphological and pose-based variations associated with DDH in a population of Japanese females and established which of these variations predict coverage. Computed tomography images of 83 hips from 47 patients were segmented for input into a correspondence-based SSM. The dominant modes of variation in the model initially represented scale and pose. After removal of these factors through individual bone alignment, femoral version and neck-shaft angle, pelvic curvature, and acetabular version dominated the observed variation. Femoral head oblateness and prominence of the acetabular rim and various muscle attachment sites of the femur and hemi-pelvis were found to predict 3D CT-based coverage measurements (R^2=0.5-0.7 for the full bones, R^2=0.9 for the joint).

Statement of Clinical Significance: Currently, clinical measurements of DDH only consider the morphology of the acetabulum. However, the results of this study demonstrated that variability in femoral head shape and several muscle attachment sites were predictive of femoral head coverage. These morphological differences may provide insight into improved clinical diagnosis and surgical planning based on functional adaptations of patients with DDH.

Keywords (5): Hip Joint; Developmental Dysplasia; Statistical Shape Modeling; Morphology; Computational Morphometrics

1 Introduction

Approximately 20% of all cases of hip osteoarthritis (OA) are attributed to developmental dysplasia of the hip (DDH), which is characterized by inadequate containment of the femoral head by the acetabulum, i.e., reduced femoral head coverage.[1] Biomechanical studies have demonstrated that patients with DDH have altered lower limb kinematics and muscle activation strategies, as well as weakness of the hip flexors, abductors, and internal rotators.[2–4] These alterations are theorized to be compensatory mechanisms which serve to provide additional stability and protection to the joint from conditions that may lead to OA.

In an effort to restore coverage and normalize hip biomechanics, patients are often treated with a periacetabular osteotomy, which is a joint preserving surgery that reorients the acetabulum to improve coverage of the femoral head. Overall, this surgery is an effective treatment for DDH.[5–7] However, suboptimal outcomes may occur when the osteotomy results in either over-coverage, leading to impingement, or under-coverage, leading to persistent hip instability.[5–9] It is therefore important to develop a complete understanding of the anatomic relationship between the femoral head and acetabulum since femoral head coverage deficiencies may be difficult to identify when subtle or localized to a specific region of the joint.[10] Most often, clinical diagnosis and surgical planning are guided by two-dimensional (2D) measurements of femoral head coverage, including the lateral center edge angle[11] (LCEA) and anterior center edge angle[12] (ACEA). However, these measurements describe the anatomy of the acetabulum and only capture femoral head coverage in a single joint orientation and radiographic projection, and thus they may fail to detect localized, and potentially subtle, deficiencies in coverage. Further, since most patients with DDH present with concomitant deformities, such as excessive femoral anteversion,[13–18] patient positioning may be altered during imaging. Such alterations in positioning could influence the appearance and prevent accurate quantification of the anatomy.

The shape variability of the hip joint in patients with DDH has also been evaluated using 2D radiographs in combination with manual landmark identification,[19–23] but these analyses suffer from similar limitations to those associated with 2D coverage measurements and cannot capture the complete morphology of the two bones. Clinical adoption of computed tomography (CT) and magnetic resonance imaging (MRI) provides the ability to quantify both global and regional coverage deficiencies and concomitant deformities in patients with DDH through 3D surface reconstructions of the anatomy.[15,24–27] While these data may enhance diagnosis and pre-operative planning, measurements made from reconstructed surfaces are generally still based on planar projections and two-dimensional imaging parameters, which do not fully capture the 3D morphology. Further complicating matters, measurements that define the spatial relationship between the femur and pelvis are likely dependent on the orientation of the participant in the CT or MRI scanner. The use of a standardized patient position during imaging could improve consistency in these measurements across participants, however some positional bias may be unavoidable.

Statistical shape modeling (SSM) applies modern computational techniques to parameterize and quantify complex anatomical shapes and their variability.[28,29] The salient advantage of SSM is that it facilitates statistical comparisons without the need for shape fitting and projection-based measurements as are often used clinically or manual identification of preconceived regions of expected variation; this increases the likelihood of identifying previously undetected group-wise differences in 3D shape. 3D SSM of the femur has been used to objectively identify the region of the proximal femur that is most affected by cam femoroacetabular impingement syndrome[30] and identify large variations in femoral version, neck-shaft angle, and femoral neck length in patients with DDH.[31] However, to date, most SSM studies that have quantified morphology of the hip joint have been limited to 2D bone contours,[19–23] which limits the ability to use these models to fully describe the specific pathology of the joint.

Recently, articulated SSMs have been developed to model human joints.[32,33] Using an articulated SSM, one can determine how the shape of the bones that comprise the joint vary across the population separate from the variation in pose of the joint. However, the utility of these models for clinical investigation of pathologies has yet to be shown and, to our knowledge, articulated SSMs have not been applied to study the pathoanatomy of DDH. The objectives of this study were therefore to: 1) apply an articulated SSM to quantify and visualize anatomic variation in both the pose and shape of the hip of patients with DDH, and 2) determine whether pose and shape variations quantified by SSM could explain variation in 3D measurements of femoral coverage.

2 Methods

Type of Study: Retrospective

Level of Evidence: III

2.1 Participants

Fifty consecutive female patients that underwent primary curved periacetabular osteotomy (CPO) for DDH between July 2008 and December 2017 were initially considered for this retrospective study approved by our Institutional Review Board. Male patients were excluded, as only a small portion of patients were male and studies have reported differences in femur and pelvis shape across sexes which could convolute analysis.[13] For each patient, hips with DDH and no evidence of advanced osteoarthritis or other morphological deformities were included, as this study focused on the prediction of coverage in individuals who would be candidates for hip joint preserving surgeries, such as periacetabular osteotomy. Therefore, hips with a LCEA > 25° (8 hips), Kellgren-Lawrence (K-L) classification of 3 or greater (6 hips), Perthes deformity (1 hip), or miscellaneous technical issues (2 hips) were excluded, leaving 83 hips from 47 patients (43 right and 40 left hips). All patients were of Asian descent and Japanese nationality with a mean ± standard deviation (SD) age, height, and mass of 37 ± 11 years, 1.58 ± 0.05 m, and 54.0 ± 8.2 kg, respectively. The mean ± SD of the LCEA measured on anteroposterior radiographs was 13.0 ± 8.0°.

2.2 Imaging and Pre-Processing

During imaging, all patients were positioned such that the pelvis was in a neutral position, legs were parallel, and knees were pointed upward. CT images were acquired with a slice thickness of 1.00 mm (78 hips, 44 patients) or 1.25 mm (5 hips, 3 patients). The full femur and hemi-pelvis of each hip were semi-automatically segmented from the volumetric images and converted to three-dimensional surfaces using Amira (v6.0.1, Visage Imaging, San Diego, CA, USA). Femur and hemi-pelvis surfaces were smoothed, aligned as a pair to eliminate global variation in rotation and translation (such that the relationship between the femur and pelvis was not altered), and reformatted to volumetric distance transforms using pre-processing tools from ShapeWorks (v5.3.1, University of Utah, Salt Lake City, UT, USA; shapeworks.sci.utah.edu).[29]

2.3 Statistical Shape Modeling

In ShapeWorks, a particle-based correspondence model of the hip joint was generated with each femur and hemi-pelvis pair representing a single hip joint. The correspondence model included 6,144 correspondence particles for each hip (n=4,096 on the femur, n=2,048 on the hemi-pelvis). From this initial *Unscaled SSM*, a two-step alignment method described by Agrawal and colleagues was used to remove variability in size and pose from the model (Figure 1).[33] In the first alignment step, hip size (i.e. scale) was normalized across the population via generalized Procrustes analysis, resulting in the *SSM with Pose*. In the second step, mean femur and hemi-pelvis shapes generated from the *SSM with Pose* were used as alignment templates to remove individual pose variations of the separate bones (femur and hemi-pelvis); these shapes were then used to generate the *SSM of Shape* (Figure 1).[33] Principal component analysis (PCA) was used to reduce the dimensionality of the correspondence model into a smaller number of modes that described dominant shape variations. PCA was applied to the correspondence model of the *Unscaled SSM* and after each step of the alignment process. Parallel analysis was used to identify the PCA modes that represented shape variance greater than random noise.[34]

2.4 Femoral Head Coverage Analysis

Femur and hemi-pelvis surfaces were reconstructed based on the mean correspondence particle configuration from the *Unscaled SSM* (Figure 1). The regions corresponding to the femoral head and lunate surface were automatically identified using 1st and 2nd principal curvature of the mean femoral head and acetabular surfaces, respectively.[35] The selected region of the lunate surface was manually adjusted to include the entire acetabular rim, as the rim is relevant to femoral head coverage, and the selection of the femoral head was expanded to include the fovea and avoid inconsistencies in fovea size and position across the population. The correspondence particles associated with the isolated regions of the joint were then used to extract the femoral head and acetabular regions from the surfaces of each patient hip in the original coordinate system of the CT images. Coverage was calculated in this orientation, as the removal of scale would not alter coverage measurements and because the final joint alignment of the two-step process was not guaranteed to place the femur and pelvis in a true anatomical orientation.

Femoral head coverage was quantified for each hip using the Area Coverage tool in ShapeWorks.[29,36] Herein, the covered region of the femoral head was defined by the nodes intersected by the normal projection of any node of the acetabular surface; thus, over-selection of the acetabular rim would not affect the results.[37] Coverage was expressed as the surface area of the covered region divided by the total surface area of the femoral head in percent.*2.5 Regression Model for Femoral Head Coverage*

PCA modes from each SSM were used to predict femoral head coverage using least absolute shrinkage and selection operator (LASSO) regression in MATLAB (R2019a, Natick, MA, USA). LASSO regression identifies a relevant, i.e. predictive, subset of variables when the initial set of variables is large.[38] PCA was run on correspondence particle coordinates of 73 hips for regression model training and validation; ten samples were randomly selected to be used in a separate test dataset and held out from the initial analysis. Eigenvalues of all 73 PCA modes were standardized to a mean of zero and a standard deviation of one. The value of the LASSO penalty term (lambda) was optimized through leave-one-out cross-validation for each regression model to isolate a subset of the PCA modes most predictive of coverage. Final regression models for the *Unscaled SSM* comprised the smallest number of PCA modes needed for the mean squared error (MSE) of predicted coverage relative to measured coverage to be within one standard error of the overall minimum MSE, i.e. one standard error rule.[39] Regression models for the *SSM with Pose* and *SSM of Shape* were limited to the number of PCA modes determined for the *Unscaled SSM* to enable direct comparison across SSMs. Final regression coefficients were obtained using a linear regression model with leave-one-out cross validation of the modes selected from LASSO. The final regression coefficients were averaged across each cross-validation model. Eigenvalues for the 10 test samples were determined from the eigenvectors of the training and validation regression model and used to evaluate the predictability of the model. The regression coefficients of each SSM were used to reconstruct predicted surfaces of minimum and maximum coverage of the cohort. Surface-to-surface distance between predicted shapes of minimum and maximum coverage were generated to visualize results.

Next, PCA and regression analysis was applied to the isolated joint correspondences to identify local shape features and isolate those that best predicted hip joint coverage. To do so, only correspondence particle locations within the regions of the femoral head and acetabulum (339 and 119 points, respectively) were included in the PCA and regression analysis for each SSM. Data were then analyzed using the same procedure described for the full bone data.

3 Results

For the initial *Unscaled SSM* (Figure 1), six PCA modes were determined to be significant and captured 95.8% of the shape variation of the full bones (60.8%, 22.9%, 5.3%, 2.7%, 2.1%, and 1.9%, for each mode respectively). For the isolated joint, four PCA modes were determined to be significant and captured 94.1% of the shape variation

(58.3%, 24.6%, 8.7%, and 2.5%, for each mode respectively). The first mode primarily represented variation in full bone scale. The second, third, and fourth modes represented variability in pose, specifically flexion-extension, abduction-adduction, and internal-external rotation, respectively. The fifth and sixth modes represented variability in the position of the joint and rotational angles of the femur and pelvis (Table 1). Similar morphological variations were observed for both the isolated joint (Figure 2) and full femur and hemi-pelvis (Figure 3).

For the globally aligned *SSM with Pose* (Figure 1), six PCA modes were determined to be significant and captured 91.7% of the shape variation of the full bones (56.7%, 13.8%, 7.1%, 6.5%, 5.0%, and 2.6%, for each mode respectively). For the isolated joint, six PCA modes were determined to be significant and captured 95.1% of the shape variation (54.4%, 21.5%, 7.6%, 5.3%, 4.3%, and 2.0%, for each mode respectively). The first, second, and fourth modes primarily represented variation in flexion-extension, abduction-adduction, and internal-external rotation, while the third, fifth, and sixth modes represented more subtle morphological variations (Table 1). Modes 1 and 2 of the *SSM with Pose* exhibited similar variation to that of Modes 2 and 3 from the *Unscaled SSM*, while Modes 4, 5, and 6 of the *SSM with Pose* represented similar variation to that captured in Modes 4, 5, and 6 from the *Unscaled SSM*. Similar morphological variations were observed for both the isolated joint (Figure 2) and full femur and hemi-pelvis (Figure 4).

For the individually aligned *SSM of Shape* (Figure 1), 11 PCA modes were determined to be significant and captured 84.4% of the shape variation of the full bones (36.0%, 13.5%, 9.4%, 5.5%, 4.3%, 3.9%, 3.6%, 2.5%, 2.2%, 1.9% and 1.5%, for each mode respectively). For the isolated joint, six PCA modes were determined to be significant and captured 91.0% of the shape variation (37.6%, 33.9%, 8.1%, 5.3%, 3.8%, and 2.3%, for each mode respectively). Compared to the *Unscaled SSM* and *SSM with Pose*, the first six modes of the full bone SSM captured 72.7% of the overall shape variation. Variation in shape captured by each PCA mode was more subtle and not easily attributed to single specific features, but did resemble those found in later modes of the *Unscaled SSM* and *SSM with Pose* (Table 1). Subtle shape variation was observed for all significant PCA modes with the variation of the joint being more localized after the first two modes (Figure 2) and the variation of the femur being qualitatively smaller in magnitude than that of the hemi-pelvis after the first three modes for the full bone model (Figure 5).

For the evaluation of coverage, the cross-validated lambda value and number of selected modes varied based on input shape data (Table 2). The number of selected modes was eight for the full bone SSMs and 13 for the joint SSMs, which represented between 6.1% and 84.9% of the overall shape variation. These findings indicate that the modes predictive of coverage were not necessarily those that described the predominate shape variation observed in each model. For the isolated regions of the joint, the variation captured by the modes selected from LASSO represented the prominence of the acetabular rim and angle of the lunate surface, as well as the flattening or oblateness of the femoral head (Figure 6, Video S-1). These features were visibly reduced for the *SSM of Shape*, however the fit of the validation data was equivalent to that of the *Unscaled SSM* and *SSM with Pose*. In addition to the features of the joint, the full bone regression model revealed that a more prominent and posterior lesser trochanter, an inferior greater trochanter, and anterior femoral bowing (Figure 7, Video S-2) were femoral features predictive of decreased coverage, while a wider iliac tilt angle, broader ischium, a more prominent anterior superior iliac spine (ASIS), and a less prominent anterior inferior iliac spine (AIIS) were pelvic features predictive of decreased coverage. These features were present in all three SSMs, however some of the more subtle features of the *Unscaled SSM* and *SSM with Pose* varied from those observed in the *SSM of Shape*, which may explain the drop in predictability for the *SSM of Shape*. Generally, the predictability of the joint level SSMs was better than that of the full bone SSMs, where the mean absolute error of prediction was 0.6% coverage for the joint SSMs and 1.1% coverage for the full bone SSMs. The predictability of the models on the 10-sample test dataset was comparable to that of the training and validation dataset (Table 2), except for the full bone *SSM of Shape* which resulted in a negative Q^2 value.

4 Discussion

An articulated SSM, which allows for analyzing variability in shape of individual bones separate from that of the pose of the joint, was applied to a population of females of Asian descent and Japanese nationality diagnosed with DDH.[33] Using this model, the relationship between femur and pelvis shape and measurements of femoral head coverage was also investigated. In both the *Unscaled SSM* and *SSM with Pose*, positional variation along the three kinematic planes of the hip (i.e., flexion-extension, abduction-adduction, and internal-external rotation) was identified in the early PCA modes, which constitute larger percentages of the total shape variation (Figures 2-4). In the *SSM of Shape*, which removed variation in scale and pose, we observed variation in the morphology of both the femur and pelvis, however the magnitude of change in femoral anatomy appeared to be reduced after the first three modes (Figure 5). Aside from anatomical differences which directly altered coverage (e.g., size and shape of the femoral head and acetabulum), a variety of less obvious morphologic features were associated with minimum and maximum measured coverage (Figure 6). Importantly, the variation in shape was not isolated to the region immediately surrounding the joint, but also included variation in the relative orientation of the ilium, ischium, and pubis, and the position of the femoral head relative to the femoral shaft (Figure 7). Additionally, muscle origin/insertion sites on both bones, including the AIIS, ASIS, and both the lesser and greater trochanters, varied with coverage which may indicate that differences in muscle recruitment or relative strength occur in parallel with variation in coverage. These findings support previous research-based and clinical observations of functional compensation in DDH patients across a broad spectrum of disease severity.[2–4]

The application of SSM to study hip morphology has been in large part limited to 2D radiographs or small regions of the joint or bone. In 2D applications, femur and pelvis shape characteristics have been identified as relevant to the incidence of OA, including modes of variation representing morphology consistent with DDH and those found herein.[19–23] To our knowledge, only one 3D SSM study evaluated the region of the joint in DDH patients and asymptomatic participants. In their study, morphological differences between males and females as well as differences associated with disease severity, such as angular steepness of the acetabular roof (i.e. lunate surface) and reduced femoral head coverage, were observed,[41] which aligns well with the morphological variation captured by our regression model of coverage. However, the region of interest in their prior study was limited to the proximal femur and distal pelvis. Another 3D SSM evaluated the full femur (interpolated from images of the proximal and distal femur) of female patients diagnosed with DDH and identified femoral version, neck-shaft angle, femoral head size, and femoral neck length as features of variation within their cohort.[31] We did not directly report shape variation for the decoupled femur, but observed similar aspects of variation for combined hip joint SSMs, even when scale and pose differences were included in the model. Previous studies have not evaluated the full hemi-pelvis of patients with DDH using 3D SSM, however a previous study evaluating morphology directly from CT images identified rotational deformities of the pelvis, including anterior or posterior rotation of the acetabulum,[17] which aligned with the morphological variation represented in Mode 4 of the *SSM of Shape*.

Decreased femoral head coverage has been shown to be independently associated with both decreased LCEA and increased acetabular retroversion.[24] Interestingly, other than the prominence of the acetabular rim, the shape variation related to coverage seemed less related to aspects of morphology thought to be associated with DDH (i.e., femoral version and neck-shaft angle) and seemed to instead align closely with muscle attachment sites (e.g. ASIS, AIIS, trochanters, posterior femur). Specifically, more prominent origin and insertion sites of the gluteus medius (lateral iliac crest and superior greater trochanter), quadratus femoris (ischial tuberosity and intertrochanteric crest), illiacus (medial iliac crest and lesser trochanter), and adductor magnus (inferior pubic ramus and medial femoral shaft) appear to be predictive of increased coverage (Figure 7), which may indicate decreased muscle lengths in patients with less severe DDH. In contrast, Liu and colleagues found that hips with dysplasia had a shorter gluteus medius than contralateral control hips, but this 7% decrease was within the standard deviation of the measurement.[42] Furthermore, in comparison to our observations, which were based on 3D bone morphology, Liu et al. relied on 2D planar measurements of muscle length, which may have been affected by muscle activation angle. In addition to the aforementioned muscles, prominent origin or insertion sites of several other muscles on the femur and pelvis associated with muscle weakness or abnormal activation in patients with DDH[2–4] were predictive of coverage in our study (i.e. anterosuperior intertrochanteric line for the piriformis and gemellus, or the AIIS and anterolateral iliac crest for the tensor fasciae latae and sartorius). This observation indicates morphological changes over the entire femur and hemi-pelvis, which are resultant of either developmental or compensatory mechanisms, may be relevant to both coverage and our understanding of DDH.

From the full bone analysis, Mode 3 from the *Unscaled SSM* and Mode 2 from the *SSM with Pose*, which both represented variation in abduction-adduction, iliac tilt angle, and other subtle morphological differences (Figures 3, 4), were found to be relevant predictors of coverage. Since our patients were positioned in a controlled manner during imaging and subtle variability in abduction-adduction is unlikely to affect overall femoral head coverage, the selection of this mode for inclusion in the predictive model may instead indicate that variation in pelvic width and iliac tilt angle were relevant to coverage. Additionally, these features also predicted coverage in the *SSM of Shape* as part of Mode 5 (Figure 5). Collectively, this exemplifies the strength of our analysis methods to identify true morphological features of coverage whether or not scale and pose were included in the model.

With respect to coverage predictions, results indicated that the morphology at the level of the joint was more predictive of coverage than consideration of the full pelvis and femur (Table 2). Similarly, the predictability of coverage from the joint SSMs was strong whether or not scale and pose were considered (Figure 6, Video S-1). The predictability from the full bone SSMs decreased with the removal of both scale and pose (Figure 7), which may indicate that more modes are necessary to accurately predict coverage due to the subtle morphological variations represented by each mode of variation for the full bone *SSM of Shape*. Additionally, interpretation of the modes when using the full bone model is challenging, highlighting the benefit of focusing an SSM on a specific region of interest to support the associated analysis.

For all SSMs, an oblate femoral head and prominent acetabular rim were predictive of coverage. Unfortunately, conventional clinical measurements, e.g., the LCEA and ACEA, rely solely on acetabular anatomy to assess coverage. Moving forward, morphology of the joint, including the femoral head, should be considered and clinical methods to measure the presence of a more oblate or larger femoral head could be helpful in assessing coverage.

This study had limitations that warrant consideration. First, our homogenous patient population was entirely female and of Asian descent and Japanese nationality, which limits the generalizability of the study results. However, our use of a homogenous population removed sources of shape variation not specifically related to DDH, such as those related to sex,[13] race and ethnicity, or unrelated deformities, such as OA-induced osteophytes. Thus, this model provided insight into the relationship between the full femur and hemi-pelvis in DDH and allowed for a systematic analysis of the morphology of the hip joint and factors related to 3D coverage in this population. Second, images were acquired with the participant supine and thus the coverage measurements reported in our study do not represent those of a functional, weight bearing position. However, we believe our measurements of coverage with the participant supine are valid and clinicallyrelatable. Notably, clinical CT and MRI scans of DDH patients are acquired supine. Furthermore, research has demonstrated that variation in pelvic tilt, which is the predominant postural difference of the hip between supine and standing in patients with DDH, does not affect coverage measurements.[43–45] Additionally, studies have demonstrated that measurements of coverage change very little when evaluated over gait.[37] Collectively, this suggests that it is largely the shape of the hip, not pose, that dictates the measurement of 3D coverage. Third, our two-step alignment approach did not specifically control the corrections in pose for the *SSM of Shape*, such that joint surfaces were not prevented from overlapping,[33] however the *SSM of Shape* was not intended to describe anatomical positions of the joint and coverage measurements were based on the CT position, so subtle overlap did not impact our analyses and conclusions.

In summary, through the use of SSM in combination with a multi-stage alignment approach, we identified pose variability to include each independent plane of hip motion and shape variability to include a number of features potentially related to biomechanical function, such as muscle attachment sites and rotational or torsional variability in the context of DDH. These factors could be related to abnormal hip biomechanics which may be a functional adaptation used to compensate for symptoms. Importantly, even within a homogeneous cohort, morphological features that were predictive of coverage measurements were found. Notably, coverage could be predicted using shape features that were present outside of the joint surfaces, which may be relevant to clinical evaluation of patients with DDH. Future studies should evaluate the observed morphological variability in the context of a more diverse study population and against asymptomatic participants to further identify morphological features directly related to symptomatic DDH. This analysis could elucidate the role biomechanics plays in the development of clinical symptoms and patient functional adaptation to hip instability.

5 Acknowledgements

We acknowledge funding from the LS Peery Discovery Program in Musculoskeletal Restoration, the Nakatomi Foundation, the Nakatani Foundation for Advancement of Measuring Technologies in Biomedical Engineering, and the National Institutes of Health under grant numbers NIBIB-U24EB029011, NIAMS-R01AR076120, NIBIB-R01EB016701, NHLBI-R01HL135568, NIGMS-P41GM103545, and NIAMS-F32AR078019. The research content herein is solely the responsibility of the authors and does not necessarily represent the official views of these funding programs.

6 References

1. Solomon L. 1976. Patterns of osteoarthritis of the hip. J. Bone Jt. Surg. - Ser. B 58(2):176–183.

2. Jacobsen JS, Hölmich P, Thorborg K, et al. 2017. Muscle-tendon-related pain in 100 patients with hip dysplasia: prevalence and associations with self-reported hip

disability and muscle strength. J. Hip Preserv. Surg. 5(1):39–46.

3. Skalshøi O, Iversen CH, Nielsen DB, et al. 2015. Walking patterns and hip contact forces in patients with hip dysplasia. Gait Posture 42(4):529–533.

4. Gaffney BMM, Van Dillen LR, Foody JN, et al. 2021. Multi-joint biomechanics during sloped walking in patients with developmental dysplasia of the hip. Clin. Biomech. 84:105335.

5. Naito M, Nakamura Y. 2014. Curved Periacetabular Osteotomy for the Treatment of Dysplastic Hips Clinics in Orthopedic Surgery • pISSN 2005-291X eISSN 2005-4408. Clin. Orthop. Surg. 6:127–137.

6. Naito M, Shiramizu K, Akiyoshi Y, et al. 2005. Curved periacetabular osteotomy for treatment of dysplastic hip. Clin. Orthop. Relat. Res. (433):129–135.

7. Lerch TD, Steppacher SD, Liechti EF, et al. 2017. One-third of Hips After Periacetabular Osteotomy Survive 30 Years With Good Clinical Results, No Progression of Arthritis, or Conversion to THA. Clin. Orthop. Relat. Res. 475(4):1154–1168.

8. Albers CE, Steppacher SD, Ganz R, et al. 2013. Impingement adversely affects 10-year survivorship after periacetabular osteotomy for DDH hip. Clin. Orthop. Relat. Res. 471(5):1602–1614.

9. Yasunaga Y, Yamasaki T, Ochi M. 2012. Patient selection criteria for periacetabular osteotomy or rotational acetabular osteotomy. In: Clinical Orthopaedics and Related Research. Springer New York LLC. p 3342–3354.

10. Nepple JJ, Wells J, Ross JR, et al. 2017. Three Patterns of Acetabular Deficiency Are Common in Young Adult Patients With Acetabular Dysplasia.475(4):1037–1044.

11. Wiberg G. 1953. Shelf operation in congenital dysplasia of the acetabulum and in subluxation and dislocation of the hip. J. Bone Joint Surg. Am. 35 A(1):65–80.

12. Lequesne M, de Seze. 1961. [False profile of the pelvis. A new radiographic incidence for the study of the hip. Its use in dysplasias and different coxopathies]. Rev Rhum Mal Osteoartic. 28:643–652.

13. Boughton OR, Uemura K, Tamura K, et al. 2019. Gender and disease severity determine proximal femoral morphology in developmental dysplasia of the hip. J. Orthop. Res. 37(5):1123–1132.

14. Fujii M, Nakashima Y, Yamamoto T, et al. 2010. Acetabular retroversion in

developmental dysplasia of the hip. J. Bone Jt. Surg. - Ser. A 92(4):895–903.

15. Hansen BJ, Harris MD, Anderson LA, et al. 2012. Correlation between radiographic measures of acetabular morphology with 3D femoral head coverage in patients with acetabular retroversion. Acta Orthop. 83(3):233–239.

16. Sugano N, Noble PC, Kamaric E, et al. 1998. The morphology of the femur in developmental dysplasia of the hip. J. Bone Jt. Surg. - Ser. B 80(4):711–719.

17. Fujii M, Nakashima Y, Sato T, et al. 2011. Pelvic deformity influences acetabular version and coverage in hip dysplasia. Clin. Orthop. Relat. Res. 469(6):1735–1742.

18. Wells J, Nepple JJ, Crook K, et al. 2017. Femoral Morphology in the Dysplastic Hip: Three-dimensional Characterizations With CT. Clin. Orthop. Relat. Res. 475(4):1045–1054.

19. Agricola R, Leyland KM, Bierma-Zeinstra SMA, et al. 2015. Validation of statistical shape modelling to predict hip osteoarthritis in females: data from two prospective cohort studies (Cohort Hip and Cohort Knee and Chingford). Rheumatology 54(11):2033–2041.

20. Barr RJ, Gregory JS, Reid DM, et al. 2012. Predicting OA progression to total hip replacement: can we do better than risk factors alone using active shape modelling as an imaging biomarker? Rheumatology 51(3):562–570.

21. Ahedi HG, Aspden RM, Blizzard LC, et al. 2017. Hip Shape as a Predictor of Osteoarthritis Progression in a Prospective Population Cohort. Arthritis Care Res. 69(10):1566–1573.

22. Mezhov V, Laslett LL, Gregory JS, et al. 2020. Predictors of total hip replacement in community based older adults: a cohort study.

23. Castaño-Betancourt MC, Van Meurs JBJ, Bierma-Zeinstra S, et al. 2013. The contribution of hip geometry to the prediction of hip osteoarthritis. Osteoarthr. Cartil. 21(10):1530–1536.

24. Kohno Y, Nakashima Y, Fujii M, et al. 2020. Acetabular retroversion in dysplastic hips is associated with decreased 3D femoral head coverage independently from lateral center-edge angle. Arch. Orthop. Trauma Surg. 140(7):869–875.

25. Larson CM, Moreau-Gaudry A, Kelly BT, et al. 2015. Are Normal Hips Being Labeled as Pathologic? A CT-based Method for Defining Normal Acetabular Coverage. Clin. Orthop. Relat. Res. 473(4):1247–1254.

26. Li L, Jia J, Zhao Q, et al. 2012. Evaluation of femoral head coverage following Chiari pelvic osteotomy in adolescents by three-dimensional computed tomography and conventional radiography. Arch. Orthop. Trauma Surg. 132(5):599–605.

27. Miyasaka D, Ito T, Imai N, et al. 2014. Three-dimensional assessment of femoral head coverage in normal and dysplastic hips: A novel method. Acta Med. Okayama 68(5):277–284.

28. Cates J, Fletcher PT, Styner M, et al. 2008. Particle-based shape analysis of multi-object complexes. In: Lecture Notes in Computer Science (including subseries Lecture Notes in Artificial Intelligence and Lecture Notes in Bioinformatics). NIH Public Access. p 477–485.

29. Cates J, Elhabian S, Whitaker R. 2017. Shapeworks: particle-based shape correspondence and visualization software. In: Statistical Shape and Deformation Analysis. Elsevier. p 257–298.

30. Harris MD, Datar M, Whitaker RT, et al. 2013. Statistical shape modeling of cam femoroacetabular impingement. J. Orthop. Res. 31(10):1620–1626.

31. Gaffney BMM, Hillen TJ, Nepple JJ, et al. 2019. Statistical shape modeling of femur shape variability in female patients with hip dysplasia. J. Orthop. Res. 37(3):665–673.

32. Audenaert EA, Van den Eynde J, de Almeida DF, et al. 2020. Separating positional noise from neutral alignment in multicomponent statistical shape models. Bone Reports 12:100243.

33. Agrawal P, Mozingo JD, Elhabian SY, et al. 2020. Combined Estimation of Shape and Pose for Statistical Analysis of Articulating Joints. In: Lecture Notes in Computer Science (including subseries Lecture Notes in Artificial Intelligence and Lecture Notes in Bioinformatics). Springer Science and Business Media Deutschland GmbH. p 111–121.

34. Horn JL. 1965. A rationale and test for the number of factors in factor analysis. Psychometrika 30(2):179–185.

35. Kapron AL, Aoki SK, Peters CL, et al. 2014. Accuracy and feasibility of dual fluoroscopy and model-based tracking to quantify in vivo hip kinematics during clinical exams. J. Appl. Biomech. 30(3):461–470.

36. Maas SA, Ellis BJ, Ateshian GA, Weiss JA. 2012. FEBio: Finite elements for biomechanics. J. Biomech. Eng. 134(1).

37. Uemura K, Atkins PR, Maas SA, et al. 2018. Three-dimensional femoral head coverage in the standing position represents that measured in vivo during gait. Clin. Anat. 31(8):1177–1183.

38. Tibshirani R. 1996. Regression Shrinkage and Selection Via the Lasso. J. R. Stat. Soc. Ser. B 58(1):267–288.

39. Hastie T, Tibshirani R, Friedman J. 2009. Model Assessment and Selection. p 219–259.

40. M H-H, TJ H, PK C, et al. 2020. Hip Kinematics During Single-Leg Tasks in People With and Without Hip-Related Groin Pain and the Association Among Kinematics, Hip Muscle Strength, and Bony Morphology. J. Orthop. Sports Phys. Ther. 50(5):243–251.

41. De Raedt S. 2015. Thesis: A Study of the Dysplastic Hip.

42. Liu R, Wen X, Tong Z, et al. 2012. Changes of gluteus medius muscle in the adult patients with unilateral developmental dysplasia of the hip. BMC Musculoskelet. Disord. 13.

43. Tani T, Takao M, Uemura K, et al. 2020. Posterior Pelvic Tilt From Supine to Standing in Patients With Symptomatic Developmental Dysplasia of the Hip. J. Orthop. Res. 38(3):578–587.

44. Tachibana T, Fujii M, Kitamura K, et al. 2019. Does Acetabular Coverage Vary Between the Supine and Standing Positions in Patients with Hip Dysplasia? Clin. Orthop. Relat. Res. 477(11):2455.

45. Uemura K, Atkins PR, Okamoto M, et al. 2020. Can measurements from an anteroposterior radiograph predict pelvic sagittal inclination? J. Orthop. Res. 38(7):1477–1485.

Figures

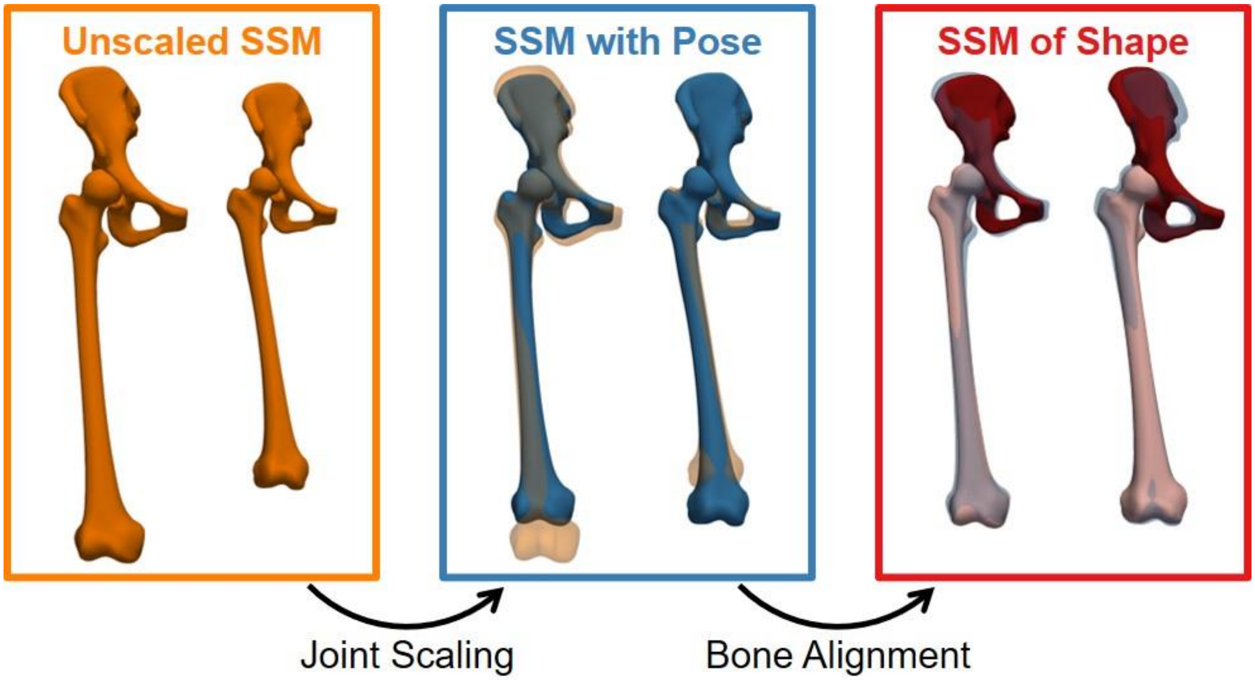

Figure 1. Stages of the statistical shape model (SSM), shown with two representative hips at each alignment stage; semi-transparent hips representing the previous alignment stage are shown for reference. An initial SSM was generated using the unscaled, globally aligned femur and hemi-pelvis data (left). Joint scaling was applied to develop models that evaluated both pose and shape (middle). Finally, bone alignment was performed to generate models of shape (right).

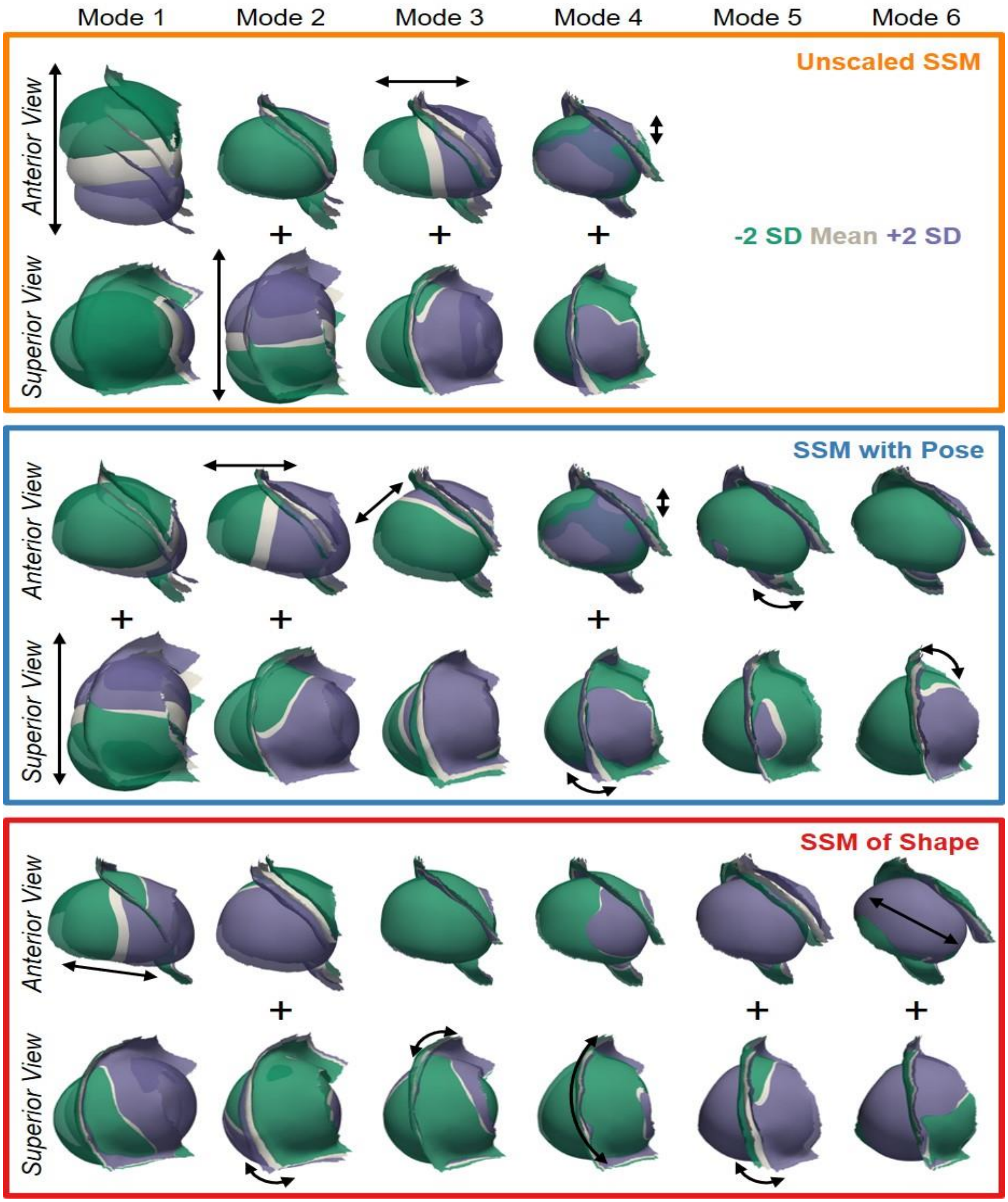

Figure 2. The principal component analysis (PCA) modes containing significant variation in shape of the *Unscaled SSM* (top), *SSM with Pose* (middle), and *SSM of Shape* (bottom). Semi-transparent surface reconstructions represent the mean and the bounds of two standard deviations for each mode from the anterior (top of each box) and superior (bottom of each box) views. Arrows qualitatively show regions of greatest variation captured by each mode. + indicates modes included in the regression model of coverage.

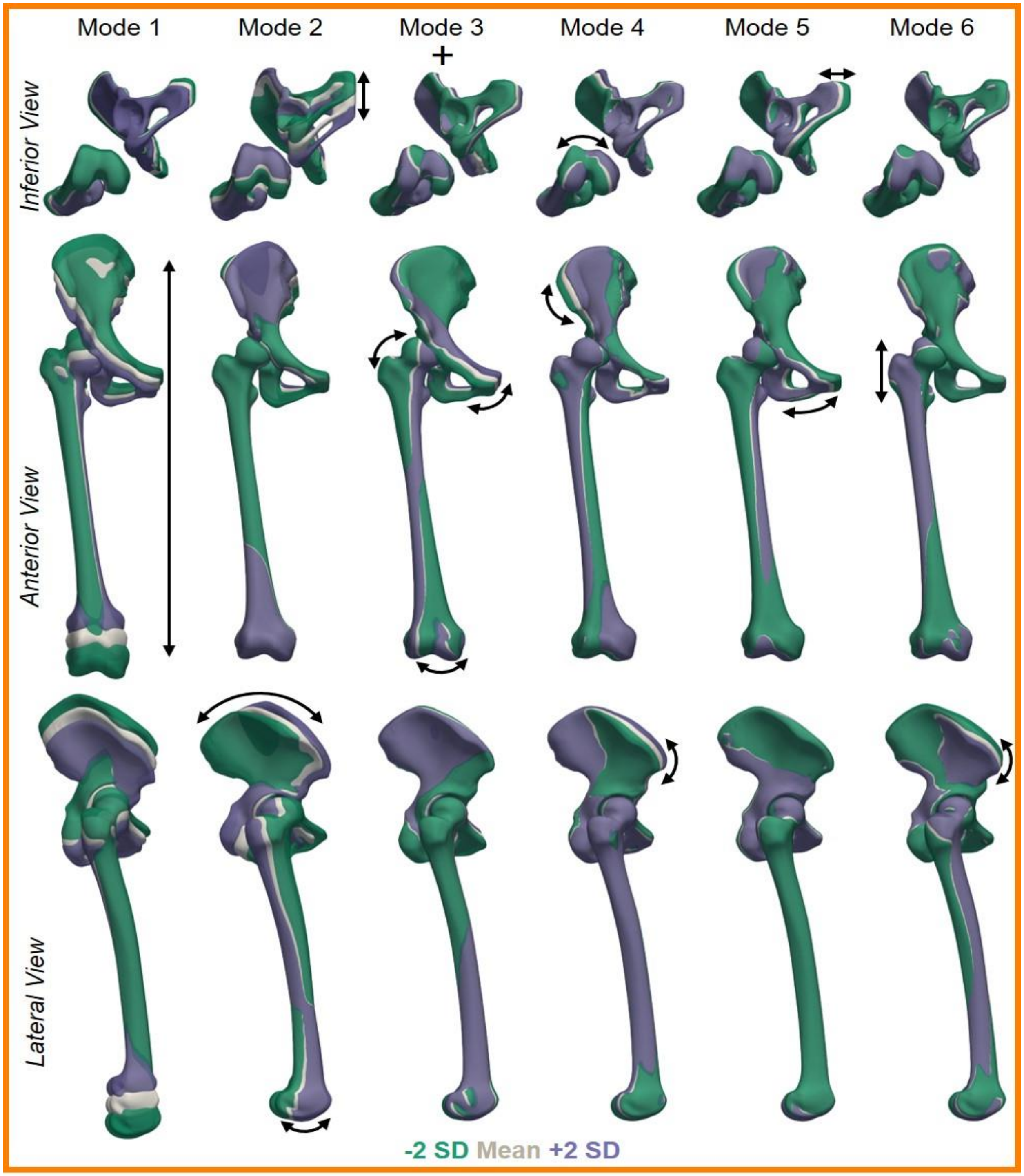

Figure 3. The first six principal component analysis (PCA) modes of the initial unscaled statistical shape model (SSM), i.e., *Unscaled SSM*, shown through semi-transparent surface reconstructions representing the mean and the bounds of two standard deviations for each mode from the inferior (top; femur and pelvis separated for visual clarity), anterior (middle), and lateral (bottom) views. Arrows qualitatively show regions of greatest variation captured by each mode. + indicates modes included in the regression model of coverage.

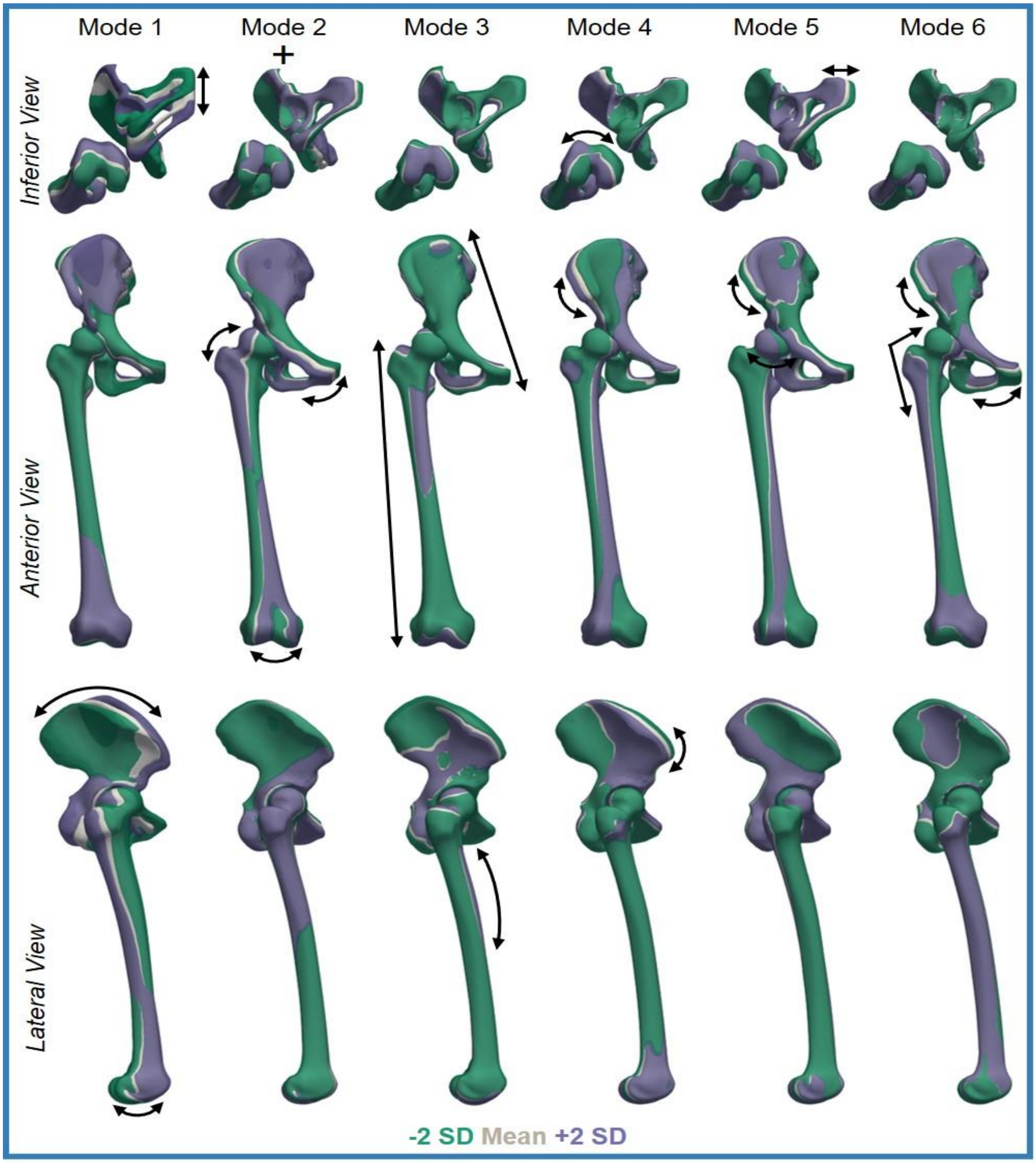

Figure 4. The first six principal component analysis (PCA) modes of the globally aligned statistical shape model (SSM) of pose and shape, i.e., *SSM with Pose*, which removed scaling and global alignment, but maintained the spatial relationship between the femur and hemi-pelvis, shown through semi-transparent surface reconstructions representing the mean and the bounds of two standard deviations for each mode from the inferior (top; femur and pelvis separated for visual clarity), anterior (middle), and lateral (bottom) views. Arrows qualitatively show regions of greatest variation captured by each mode. + indicates modes included in the regression model of coverage.

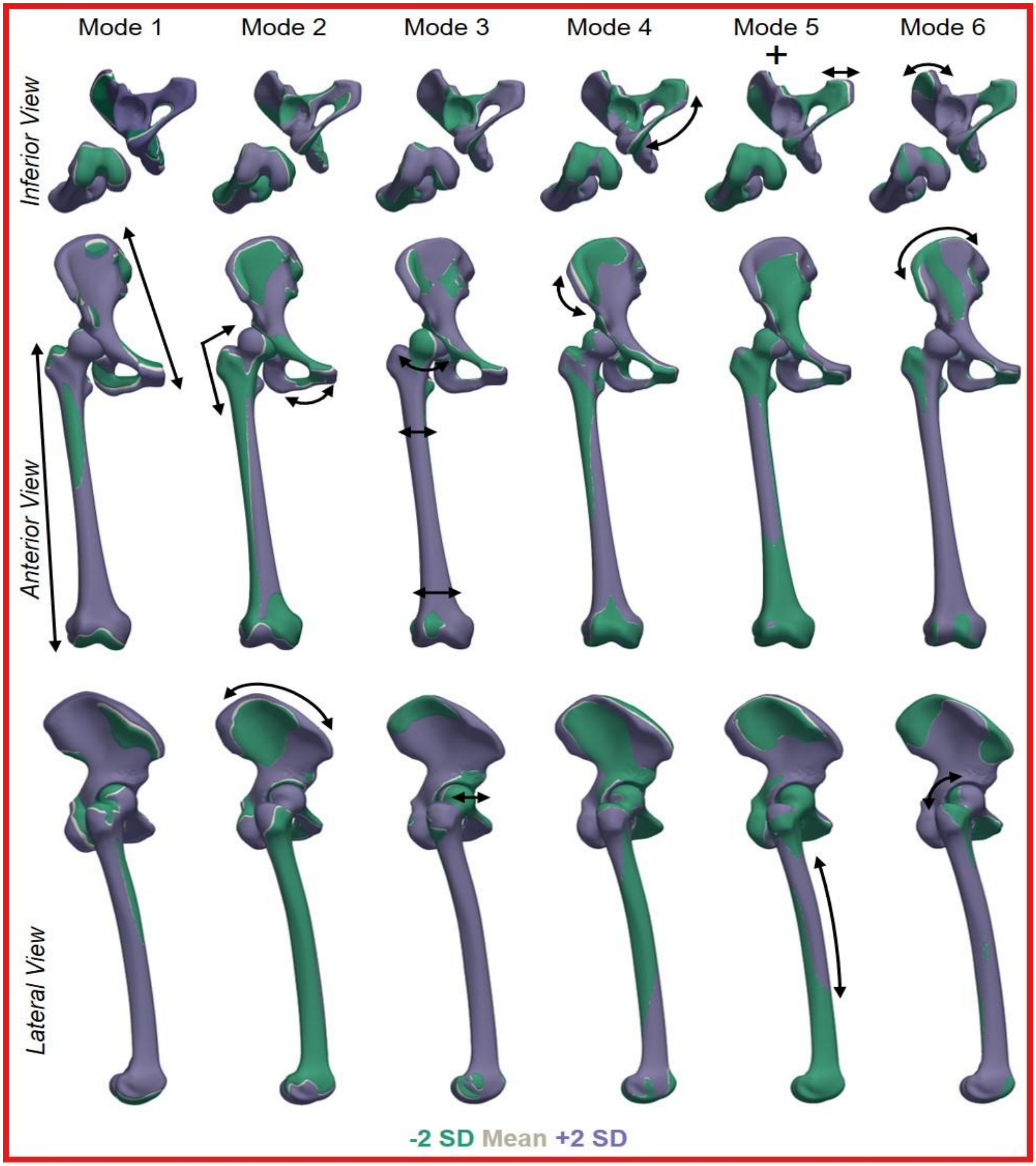

Figure 5. The first six principal component analysis (PCA) modes of the individually aligned statistical shape model (SSM) of bone shape, i.e., the *SSM of Shape*, which removed the relative relationship between orientation of the femur and pelvis, shown through semi-transparent surface reconstructions representing the mean and the bounds of two standard deviations for each mode from the inferior (top; femur and pelvis separated for visual clarity), anterior (middle), and lateral (bottom) views. Arrows qualitatively show regions of greatest variation captured by each mode. + indicates modes included in the regression model of coverage.

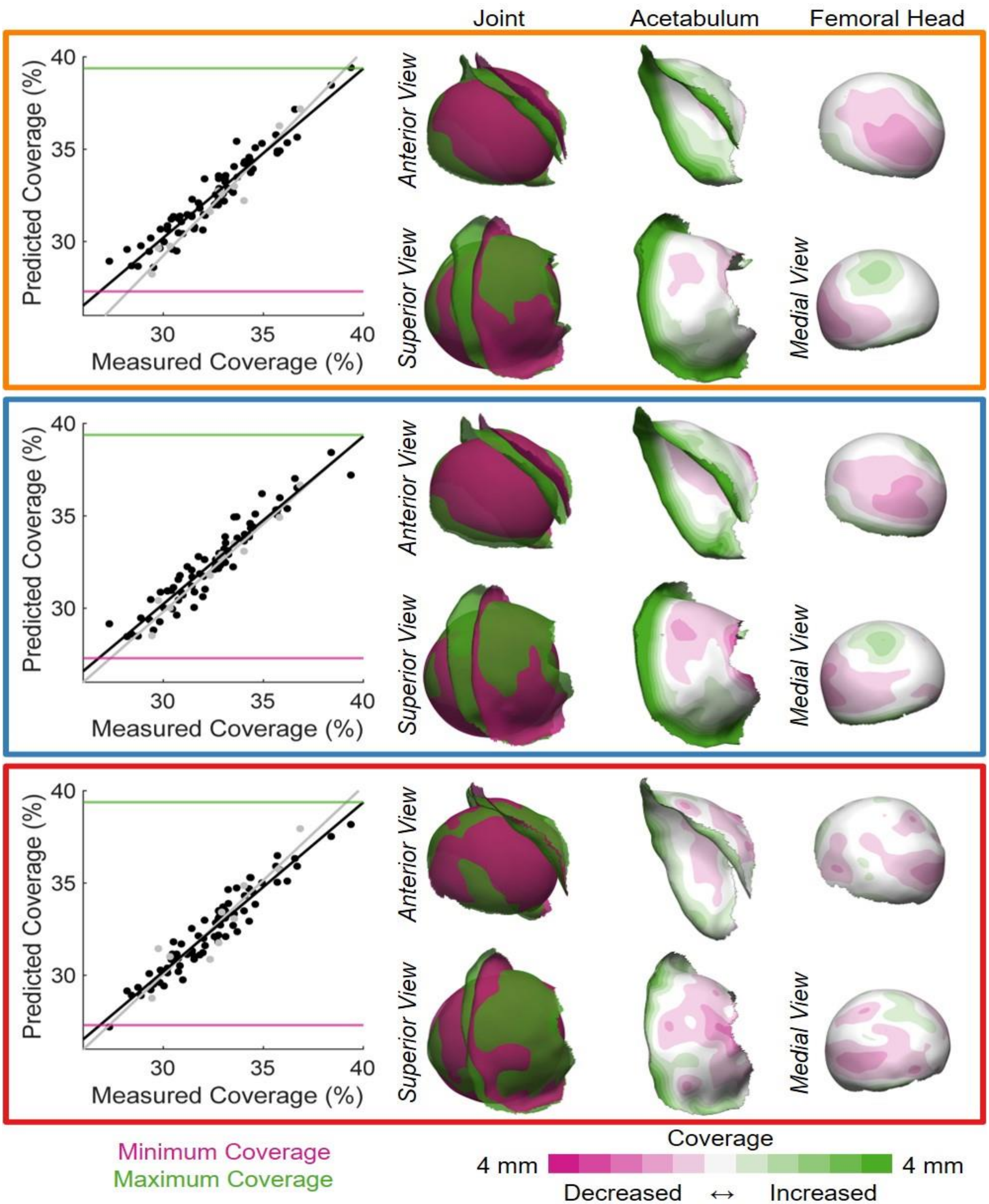

Figure 6. Linear regression model predictions of coverage (left inscribed plots) for each SSM: *Unscaled SSM* (top), *SSM with Pose* (middle), and *SSM of Shape* (bottom);

including semi-transparent surface reconstructions (center; “joint”) and surface distance plots (right; “acetabulum” and “femoral head”) of predicted minimum and maximum coverage. Linear regression-based predictions of coverage for test data are shown in gray with training and validation data in black; the line of best fit for each dataset and horizontal lines of minimum and maximum coverage are shown. Semi-transparent surface reconstructions show the predicted shapes for minimum and maximum coverage values of the population. Surface distance plots represent regions indicative of increased and decreased coverage as shown on the surface of maximum coverage. Differences in oblateness of the femoral head, prominence of the acetabular rim, and curvature of the lunate region were identified for all models.

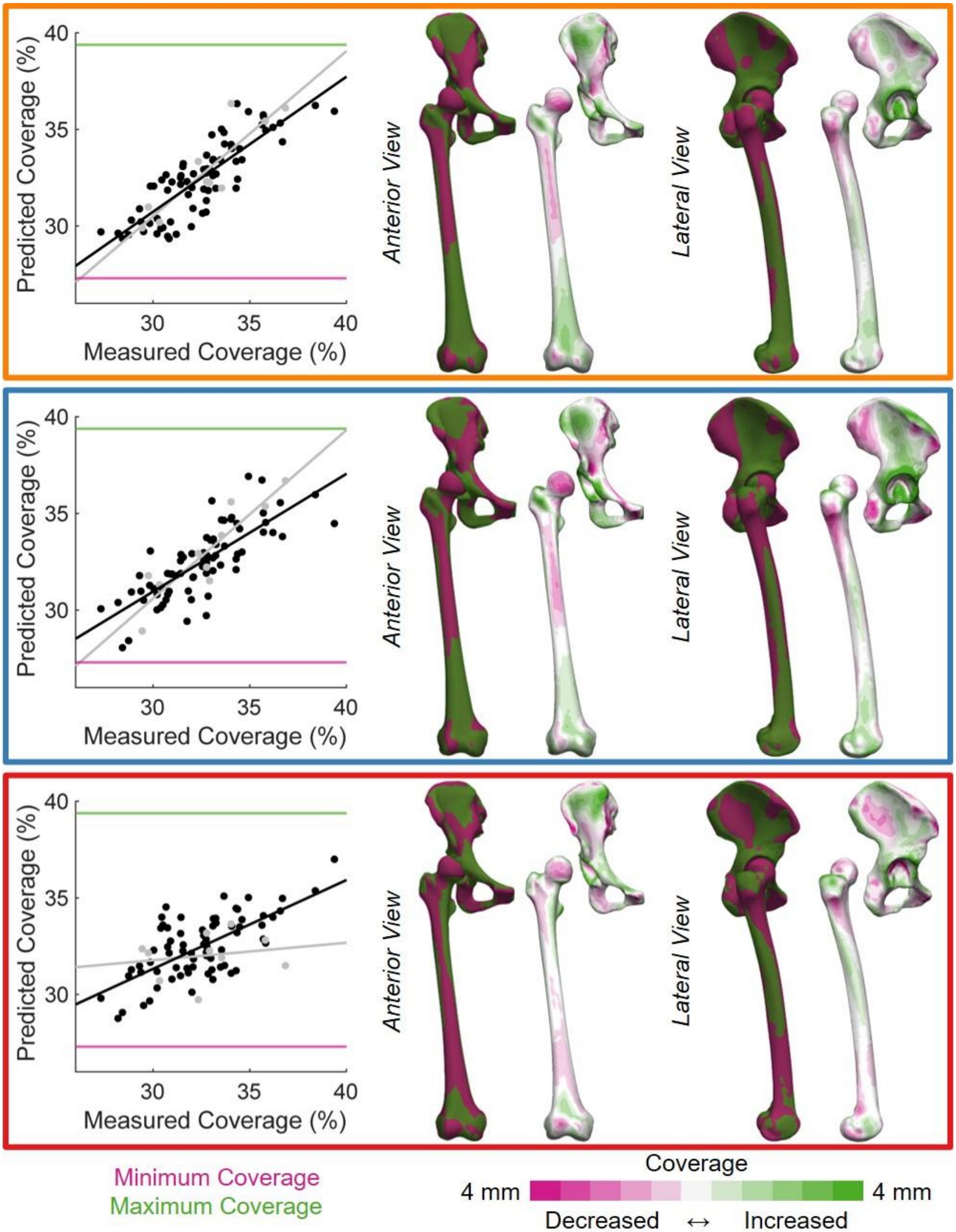
Predicted Coverage (%)
Measured Coverage (%)
Anterior View
Lateral View
Minimum Coverage
Maximum Coverage
Coverage
4 mm
4 mm
Decreased ↔ Increased

Figure 7. Linear regression model predictions of coverage (left inscribed plots) for each SSM: *Unscaled SSM* (top), *SSM with Pose* (middle), and *SSM of Shape* (bottom); including semi-transparent surface reconstructions and surface distance plots (right) of predicted minimum and maximum coverage of the femur and hemi-pelvis. Linear regression-based predictions of coverage for test data are shown in gray with training and validation data in black; the line of best fit for each dataset and horizontal lines of minimum and maximum coverage are shown. Semi-transparent surface reconstructions show the predicted shapes for minimum and maximum coverage values of the population. Surface distance plots represent regions indicative of increased and decreased coverage as shown on the surface of maximum coverage. Differences in oblateness of the femoral head and prominence of the acetabular rim and various muscle attachment sites are visible.

Tables

Table 1. Description of dominant variations observed for the modes visualized in Figures 2-5.

Mode	*Unscaled SSM*	*SSM with Pose*	*SSM of Shape*
1	Scale	Flexion-extension (pelvic tilt angle)	Relative scale of femur and pelvis, femoral bowing
2	Flexion-extension (pelvic tilt angle)	Abduction-adduction (iliac tilt angle), distal femoral version	Femoral neck-shaft angle, iliac thickness and curvature
3	Abduction-adduction (iliac tilt angle), femoral version, pelvic twist	Relative scale of femur and pelvis, ilium angle, femoral bowing	Bone thickness, femoral version
4	Internal-external rotation (iliac opening angle), ilium angle	Internal-external rotation (iliac opening angle)	Iliac-ilium angle, femoral neck-shaft angle
5	Pelvic width, femoral offset and neck-shaft angle	Proximal femoral version, pelvic width	Femoral bowing, iliac crest curvature, pubic symphysis position

6	Illiac angle, femoral version, superior-inferior joint position	Femoral neck-shaft angle, ilium position, iliac thickness and curvature	Iliac curvature, femoral version

Table 2. Regression parameters for the prediction of femoral head coverage from PCA mode data and the resultant prediction results for the training and test datasets for different input shape data sets from each SSM.

Shape Data	Lambda	Ranked Modes (Number of Modes, Percent Variance Captured)	Training		Test	
			R^2	MAE	Q^2	MAE
Unscaled SSM	0.0040	19, 12, 3, 32, 23, 28, 20, 13 (8 Modes, 6.1%)	0.70	1.1	0.79	0.9
SSM with Pose	0.0043	18, 11, 2, 14, 23, 32, 28 (7 Modes, 15.0%)	0.61	1.1	0.81	0.9
SSM of Shape	0.0048	35, 11, 28, 27, 7, 15, 5 (7 Modes, 11.5%)	0.46	1.4	-0.12	2.0
Unscaled SSM	0.0023	12, 11, 6, 4, 13, 7, 9, 2, 3, 16, 17, 8, 21 (13 Modes, 39.6%)	0.92	0.6	0.89	0.6
SSM with Pose	0.0024	11, 12, 8, 9, 4, 10, 2, 1, 18, 17, 16, 13 (12 Modes, 84.9%)	0.91	0.6	0.94	0.5

SSM of Shape	0.0024	9, 5, 6, 8, 10, 13, 16, 43, 47, 14, 2, 19, 29 (13 Modes, 44.0%)	0.92	0.6	0.83	0.9

Abbreviation: MAE, mean absolute error, presented as percent coverage; SSM, statistical shape model.